Semiconductor Physics, Quantum Electronics & Optoelectronics, 2022. V. 25, No 3. P. 262-274.

Semiconductor physics

Short-time dynamics of noise-induced escapes and transitions in overdamped systems

S.M. Soskin,[1]* V.I. Sheka,[1] T.L. Linnik,[1,2] and R. Mannella[3]

[1] *V. Lashkaryov Institute of Semiconductor Physics, National Academy of Sciences of Ukraine, 03680 Kyiv, Ukraine*
[2] *Experimentelle Physik 2, Technische Universitat Dortmund, 44227 Dortmund, Germany*
[3] *Dipartimento di Fisica, Università di Pisa, 56127 Pisa, Italy*
**Corresponding author e-mail: stanislav.soskin@gmail.com*

Abstract. Using the path-integral approach, we have developed a general solution of the problem of a noise-induced escape or transition of the overdamped one-dimensional potential system at time scales of the order of dynamic relaxation time. The results strongly differ from those obtained before by other methods. Computer simulations confirm the validity of our theory in the relevant time range. The obtained results may be of interest in studies of Josephson junctions, levitating nanoparticles in optical traps, ionic channels, chemical reactions and chemical-physical systems.

Keywords: one-dimensional potential system, short-time dynamics, noise-induced escape, overdamped system, path-integral approach.

https://doi.org/10.15407/spqeo25.03.262
PACS: 02.50.-r, 05.40.-a, 05.20.-y, 82.40.Bj

Manuscript received 02.08.22; revised version received 19.09.22; accepted for publication 21.09.22; published online 06.10.22.

1. Introduction

The overdamped stochastic equation is commonly defined as [1]

$$\frac{\mathrm{d}x}{\mathrm{d}t} = -\frac{\mathrm{d}U(x)}{\mathrm{d}x} + f(t), \qquad \langle f(t)\rangle = 0,\ \langle f(t)f(0)\rangle = 2D\,\delta(t). \tag{1}$$

Such a model may be relevant to various systems, *e.g*. Josephson junctions [2], optical systems [3, 4], levitating nanoparticles [4, 5], ionic channels [6–8], chemical reactions of a single molecule [9–11], and chemical-physical systems [12].

Beginning of theoretical studies on ovedamped stochastic processes dates back to the celebrated works by Einstein [13, 14] who studied the Brownian motion of a free particle, which may formally be considered as an overdamped motion in a parabolic potential with velocity as the generalized coordinate. A more general study of overdamped stochastic processes was started by Smoluchowski [15] who formulated the equation of motion for the probability density in an arbitrary overdamped system. This equation bears his name nowadays. The next milestone was the work by Kramers [9] who, in particular, formulated the problem of noise-induced *escape* of an overdamped system from a metastable potential well and derived its quasi-stationary solution. The expression for quasi-stationary escape flux was found in [9] using the relevant stationary solution of the Smoluchowski equation:

$$J_{qs} = A_{qs} e^{-\frac{\Delta U}{D}},\ D << \Delta U, \tag{2}$$

where ΔU is the potential barrier assumed to be much less than the noise intensity D and A_{qs} is the prefactor, which weakly depends on D as compared to the exponential (activation) factor, respectively.

The escape flux becomes quasi-stationary when time greatly exceeds the characteristic time of the formation of quasi-equilibrium within the major part of the metastable well, $t_{qe} \sim t_r \ln(\Delta U/D)$, where t_r is the characteristic relaxation time. But what is the escape flux $J(t)$ on time scales $t \le t_{qe}$? Such a question becomes relevant e.g. in the case when noise acts on the system only during a short time. The relevance of short time scales for real experiments and applications grows as modern technologies develop.

There were only a few theoretical works on the escape in overdamped systems on time scales $t \le t_{qe}$. One of the most general works was the one by Shneidman [16], who solved the non-stationary Smoluchowski equation for an arbitrary potential using the Laplace integral transformation method under assumption of quasi-equilibrium formed in the vicinity of the bottom of the well. This assumption is valid only for times significantly exceeding the relaxation time t_r, while the results of [16] are incorrect for shorter times. The present work covers the latter range by using the path-integral method [17–20], sometimes called also the method of optimal fluctuation [21]. We note also that, unlike [9, 16], our theory may be valid for large D too.

In parallel to the development of the *escape* problem on short times, there was an interesting discussion in the 90th [22–24] on the *transition* problem on short times. This problem may be of interest in the context of prehistory probability density [25], ionic channels [6–8] and some biological problems [26, 27]. Unlike the case of escape, both the initial and final points of transition differ from the stationary points of a noise-free system. Moreover, if they lie within the same monotonous part of the potential, the transition may possess features distinctly different from those of the escape. Therefore, basing on the *optimal fluctuation* method [17, 21], the authors of [22] suggested that the *most probable transition path* (MPTP) for a short-time transition uphill the slope of the potential barrier may first relax close to the bottom of the well and only then go to the final point. They supported their suggestion by analytic calculations for the parabolic approximation of the potential well and, seemingly, by numerical calculations for the exact potential. However, it was shown in [23] (also by numerical calculations using the optimal fluctuation method) that the path, which first climbs up close to the barrier top and only then relaxes to the final point, may provide an exponentially larger activation factor. Therefore, just the latter path pretends to be the MPTP in such a case. Is it possible to resolve this problem rigorously? If yes, may the MPTP possess more than one turning point? And may the MPTP switch its form jump-like as the transition time varies? Our *present* work answers all these questions too. It should be also noted that, apart from being necessary for calculation of the activation energy, MPTP may be of interest on its own. For example, in the problem of optimal control, the MPTP determines the dynamics of the external force, which optimally enhances or suppresses a given fluctuational transition [28, 29].

We also verify the theoretical results by computer simulations. Preliminary results of our work were presented in the proceedings [26, 30].

The structure of the paper is as follows. Sec. 2 presents basic equations of the path-integral method and the general results of the application of this method to the problem of interest, including formal expressions for the MPTP, activation energy and prefactor. We also describe in Sec. 2 the simulation setup. Sec. 3 presents the detailed theoretical analysis for a few characteristic cases, separately for the escape and transition problems. For some of these cases, the theoretical results are compared with the results of simulations. Conclusions are given in Sec. 4.

2. Basic concepts and general scheme

A fundamental quantity for any fluctuational problem is the transition probability density $P(x_0, x_f, t)$ [1]. $P(x_0,x_f,t)dx$ is the probability for the coordinate x, being initially equal to x_0, to be in the interval $[x_f\,;\, x_f + dx]$ at the instant t. All major physical quantities related to the transition may be expressed *via* $P(x_0, x_f, t)$ [1] (or, equivalently, *via* the prehistory probability density [25]). The quantity of the major interest in the present paper (and in most of applications) is the probability flux [1]:

$$J\left(x_0, x_f, t\right)=\left[-\frac{dU\left(x_f\right)}{dx_f}-D\frac{d}{dx_f}\right]P\left(x_0, x_f, t\right). \qquad (3)$$

We shall call it the non-stationary *escape* or *transition* flux if the initial coordinate coincides or does not coincide with the bottom of the potential well, respectively.

2.1. Activation factor

In the asymptotic limit of small noise intensities, $D \to 0$, the leading dependence on D of any physical quantity related to the noise-induced transition is activation-like [17–21]. This can be easily understood from the following reasons. The white noise $f(t)$ (1) may be characterized by the probability functional $P_{wn}(f)$ [17] (which determines the probability density in the functional space for a given realization $[f(\tau)]$ in a given time interval $[t_0,t_f]$) in the following form:

$$P_{wn}\left[f(\tau)\right] \propto \exp\left[-\frac{1}{4D}\int_{t_0}^{t_f} d\tau\, f^2(\tau)\right]. \qquad (4)$$

Due to the smallness of D, the exponential function in (4) depends very sharply on $[f(\tau)]$. Therefore, it is intuitively obvious and can be rigorously shown [17–21] that the leading dependence of $P(x_0, x_f, t = t_f - t_0)$ on D is determined by realizations of $[f(\tau)]$ close to the one, which provides the maximum value of the exponent in (4) when the given transition $x_0 = \xrightarrow{t_0 \to t_f} x_f$ takes place. As a consequence [17–23],

$$P\left(x_0, x_f, t \equiv t_f - t_0\right) = B(D,t)e^{-\frac{S_a(t)}{D}}, \qquad (5)$$

where S_a is called *activation energy* and is equal to the minimum of the functional called *action*:

$$S_a = \min_{[x(\tau)]} S\,, \quad S \equiv S\left[x(\tau)\right] = \int_0^t d\tau\, L(x,\dot{x}),$$

$$L = \frac{1}{4}\left(\dot{x} + \frac{dU}{dx}\right)^2, \quad x(0) = x_0\,, \quad x(t) = x_f \qquad (6)$$

(the same activation energy is obviously relevant to the flux J (3)) and $B(D, t)$ is called *prefactor*, respectively. The dependence of the latter on D for small D values is much weaker than that of the activation factor $\exp(-S_a/D)$. The prefactor will be considered in the next subsection. Here, we consider in more detail the activation factor and related quantities.

The necessary condition for the minimum of the functional S (6) is zero variation and, as a consequence, satisfaction of the Euler equation [22, 31] for the *most probable transition path* $[x(\tau)]$:

$$\ddot{x} - \left(dU/dx\right)\left(d^2U/dx^2\right) = 0\,. \qquad (7)$$

Solutions of Eq. (7) satisfying the boundary conditions from Eq. (6) are called *extreme* paths. They

provide extrema of the action S in the functional space. Some of extreme paths were numerically found in [22, 23] for the double-well Duffing potential and various sets (x_0, x_f, t). We provide the analysis of extreme paths and corresponding actions S in a more explicit form, which allows us to predict and analyze characteristic cases not considered in [22, 23]. Besides, we use the theorem proved in [32] stating that the number of turning points in MPTP, *i.e.* in the solution of Eq. (7), which provides the *absolute* minimum of action cannot exceed 1 that drastically reduces the number of paths eligible for being the MPTP.

Eq. (7) possesses the first integral [31], which, by analogy with the mechanics [33], may be called *quasi-energy*:

$$E = \dot{x}\left(\partial L/\partial \dot{x}\right) - L = \left(\dot{x}^2 - \left(dU/dx\right)^2\right)\big/4 . \tag{8}$$

Note that Eq. (7) coincides with the Newton equation describing the mechanical motion in an auxiliary potential $\tilde{U}(x) = -(dU/dx)^2/2$, from which the constancy of E (8) is also obvious. Note, however, that E in Eq. (8) is twice as small as the mechanical energy related to the Newton equation (7). It follows from (8) that

$$\dot{x} = \pm\sqrt{4E + \left(dU/dx\right)^2} , \tag{9}$$

where the sign is specified by the sign of the initial velocity and the number of turns preceding a given instant.

Given that $\dot{x}^2$ cannot be negative, it follows from (8) that E should necessarily satisfy the following condition:

$$E \geq E_{\min} \equiv -\min_{[x_0, x_f]}\left[\left(dU/dx\right)^2/4\right]. \tag{10}$$

One can easily separate variables in (9) and present the solution in terms of quadratures for any E in the range (10). In Sec. 3, we consider separately the transitions following stationary points of the noise-free system and those avoiding them. $S_a(t)$ and the evolutions of the MPTP significantly differ in these two cases. Furthermore, in the two subsections below, we describe in general terms the prefactor and the simulation setup.

2.2. Prefactor

There are some equivalent schemes for calculation of prefactor using the path-integral method [17–21]. We use the scheme derived in [18] for some particular case and extended for a more general case in [20]. Within this scheme, the probability density is expressed by the following expression [20]:

$$P\left(x_0, x_f, t\right) = \frac{\exp\left(S_a/D\right)}{\sqrt{4\pi DQ}}\left[1 + O(D)\right] , \tag{11}$$

where the auxiliary quantity $Q \equiv Q(x_0, x_f, t)$ is the result of integration of the certain second-order linear differential equation with the certain initial conditions, namely

$$\frac{\mathrm{d}^2 Q}{\mathrm{d}\tau^2} + \frac{\mathrm{d}Q}{\mathrm{d}\tau}\left\{2\frac{\mathrm{d}^2 U(x)}{\mathrm{d}x^2}\right\} + Q\left\{\frac{\mathrm{d}^3 U(x)}{\mathrm{d}x^3}\left(\frac{\mathrm{d}x}{\mathrm{d}\tau} - \frac{\mathrm{d}U(x)}{\mathrm{d}x}\right)\right\} = 0 ,$$

$$Q(\tau = 0) = 0 , \quad \frac{\mathrm{d}Q(\tau = 0)}{\mathrm{d}\tau} = 1 , \tag{12}$$

Here, $x \equiv x(x_0, x_f, \tau)$ is the most probable transition path. Eq. (12) assumes that the absolute minimum of action is sufficiently deeper than its other possible local minima, so that the contributions from the latter may be neglected. Otherwise, summation must be done over all relevant local minima.

Substituting Eq. (12) into Eq. (3) and using the property [20]

$$\partial S_a/\partial x_f = \left(\mathrm{d}x/\mathrm{d}\tau\big|_{\tau=t} + \mathrm{d}U\left(x_f\right)/\mathrm{d}x_f\right)\big/2 , \tag{13}$$

where $x = [x(\tau)]$ is the MPTP, one can obtain the expression for the flux J. Therefore, to the lowest order in D, the flux is described by the following formula:

$$J^{(0)}\left(x_0, x_f, t\right) \approx \frac{1}{2}\frac{\mathrm{d}x}{\mathrm{d}\tau}\bigg|_{\tau=t}\frac{\exp\left(S_a/D\right)}{\sqrt{4\pi DQ}} . \tag{14}$$

Eq. (14) has a clear interpretation. The flux at the point x_f is equal to the product of the velocity on the MPEP at x_f and the probability density at x_f multiplied by the factor 1/2. The latter arises due to the possibility for the system to cross x_f in the backward direction. No factor 1/2 in the expression for the flux would be present if there was an *absorbing* wall at x_f, similar to the case of the quasi-stationary flux [16].

2.3. Simulation setup

To obtain the flux from computer simulations, we use the following scheme. We put the system in $x = x_0$ and integrate the stochastic equation until a given time limit t_i is reached. The time limit t_l should be chosen larger than the time of the formation of a quasi-stationary flux, which is checked in the end, when $J(t)$ is derived. Then the system is reset to the bottom and everything is repeated. After sufficient statistics is collected, the flux is calculated as

$$J(t) = \left(N_{res}\right)^{-1}\frac{\Delta N_+(t) - \Delta N_-(t)}{\Delta t} \tag{15}$$

where N_{res} is the overall number of resets and $\Delta N_+(t)$ and $\Delta N_-(t)$ are the numbers of crossings of x_f during a short interval $[t, t + \Delta t]$ in the positive and negative direction, respectively. The interval Δt should be chosen small compared with any relevant time scale but large enough for $\Delta N_{\pm}(t)$ to greatly exceed 1.

Simulations for obtaining the probability density are similar. The probability density is calculated by the following expression:

$$P(x_0,x,t)=(N_{res})^{-1}\frac{\Delta N_x(t)}{\Delta x}, \qquad (16)$$

where Δx is a small interval of x and $\Delta N_x(t)$ is the number of resets such that the coordinate of the system turns out in the interval $[x, x+\Delta x]$ at the instant t.

3. Detailed results

3.1. Escape problem

The escape problem is typically defined as that with the initial state at the bottom of the well, $x_0 = x_w$ (this is the most natural initial state in which the system stays in the absence of noise), while the final coordinate x_f is at the top of the barrier, x_b, or beyond it, for example at the bottom of the neighboring well (cf. Fig. 1a).

It follows from Eq. (10) that $E_{\min} = 0$ if the interval $[x_0, x_f]$ contains at least one stationary point (*i.e.* the point where $dU/dq = 0$). Therefore, the quasi-energy E for the solution of the Euler equation for the escape problem is necessarily non-negative. This means in its turn that the extreme path $[x(\tau)]$ cannot have turning points. The integration of Eq. (9) results in

$$\tau(x)=\int_{x_w}^{x} dq\, z(q,E),$$

$$z(q,E)\equiv \mathrm{sign}\left[x_f-x_0\right]\frac{1}{4E+\left(dU(q)/dq\right)^2},$$

$$x\in\left[x_w,x_b\right], \qquad (17)$$

where the quasi-energy E is determined from the final condition

$$t=\int_{x_w}^{x_f} dq\, z(q,E). \qquad (18)$$

The function $t(E)$ (18) monotonously decreases from ∞ to 0 as E increases from 0 to ∞, provided dU/dx is analytic at $x = x_{st}$. Therefore, for each given t, there is only one value of E satisfying the expression (18). Hence, there is only one extreme path (17). To distinguish this case from the case of transitions, we call the path (17) the most probable *escape* path (or MPEP). The action along it constitutes the *activation energy* S_a for the escape. By analogy with classical mechanics [33],

$$\partial S_a/\partial t=-E\,. \qquad (19)$$

Taking into account that $E > 0$, we conclude that the activation energy S_a is a monotonously decreasing function of the transition time t.

Quantitative evaluation of the activation energy (6) can be significantly simplified by using Eq. (9) and the transformation of variables $d\tau = dx/\dot{x}$. S_a is reduced to the following quadrature:

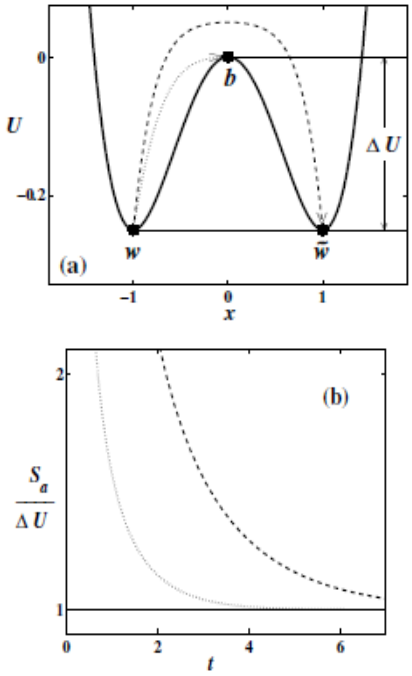

Fig. 1. (a) The Duffing potential $U(x) = -x^2/2 + x^4/4$ (thick solid line) and schematic pathways of the escape from the left well (dotted line) and the inter-well transition (dashed line). Dots mark the minima of the potential wells and the top of the barrier. (b) Time dynamics of the normalized activation energy for the escape (dotted line) and the inter-well transition (dashed line) calculated using Eq. (20). The asymptotic large-time value is shown by the solid line.

$$S_a(t)=\int_{x_0}^{x_f} dq\,\eta(q,E(t)),$$

$$\eta(q,E)=\frac{1}{2}\left(\frac{\mathrm{sign}\left[x_f-x_0\right]\left(2E+\left(dU/dq\right)^2\right)}{\sqrt{4E+\left(dU(q)/dq\right)^2}}+\frac{dU}{dq}\right), \qquad (20)$$

where $E = E(t)$ is implicitly given by (18).

Generally speaking, the integral in (20) should be evaluated numerically. However, it is much easier to do this than to numerically solve either the minimization problem (6) or even Eq. (7) with further numerical evaluation of the action integral over time as in [22, 23]. Besides, some conclusions may be drawn even without explicit integrating in Eq. (20). In particular, changing the variables $q \to U$ in (20), it is easy to show that for the transition from the bottom of the potential well x_w, to the top of the potential barrier x_b

$$S_a(t\to\infty)=\Delta U\equiv U(x_b)-U(x_w)\,, \qquad (21)$$

which obviously agrees with the conventional formula (2) for the quasi-stationary escape [9].

Fig. 1a shows the Duffing potential used in [22–24]:

$$U(x)=-x^2/2+x^4/4\,. \qquad (22)$$

Fig. 1b shows the dynamics of the activation energy for two types of escapes, namely to the top of the barrier and to the bottom of another well (the latter type may be also called the inter-well transition). The dynamics of S_a in these two cases are closely related to each other:

$$\Delta S_a\left(w \overset{t}{\to} \tilde{w}\right) = 2\Delta S_a\left(w \overset{t/2}{\to} b\right),$$

$$\Delta S_a \equiv S_a - \Delta U\,, \quad \Delta U \equiv U(x_b) - U(x_w)\,. \tag{23}$$

Knowing the MPEP and the activation energy, we may calculate to the lowest order in D both the probability density and the flux using respectively Eqs. (11) and (14). The flux calculated by this method for the Duffing oscillator (22) is shown in Fig. 2. In the short-time range, $t \le t_r \equiv 1$, it agrees well with the flux derived from the simulations, in contrast to the Shneidman theory [16], the predictions of which drastically differ from the simulation results.

Assuming that the first-order (in D/S_a) correction in the probability density is equal to zero, the first-order correction to the flux $J^{(0)}(t)$ reduces to

$$\Delta J^{(1)}(t) = \frac{1}{2} D \frac{\partial \ln(Q)}{\partial x_b} \frac{\exp\left(-S_a/D\right)}{\sqrt{4\pi DQ}}\,. \tag{24}$$

This expression nicely describes the simulation results up to $t \sim 3 \equiv t_{qe}$. However, the underlying assumption is not obvious. It is a challenging problem either to rigorously prove it or, otherwise, to find the true first-order correction to the probability density.

3.2. Transition problem

Let the initial and final points are within the same monotonous part of a potential curve $U(q)$. From the academic point of view, this case is more interesting than just the escape from the bottom and namely it was in the focus of the discussion in literature a few years ago [22–24]. Apart from the academic interest, this case may be also interesting in the context of the problem of prehistory probability density [25] and of some biological applications [26, 27].

3.2.1. Activation factor

In terms of our rigorous theory, non-triviality of the transition case is a consequence of the fact that the minimum energy $E_{\min}$ (10) is *negative* rather than equal to zero. The extrema with negative energies may possess turning points. We present below rigorous general consideration of the activation factor. We illustrate it by the example discussed in [22–24] as well as by some other characteristic examples where the situation may be more complicated than it was assumed in [22–24]. In particular, the criterion for large transition times t derived in [23] based on numerical calculations and intuitive arguments may turn out invalid for shorter times, so that a jump-like switch may occur between the MPTPs of different topologies as time t varies. In the end of this sub-subsection, we formulate a general algorithm of the analytic search for the MPTP and activation energy.

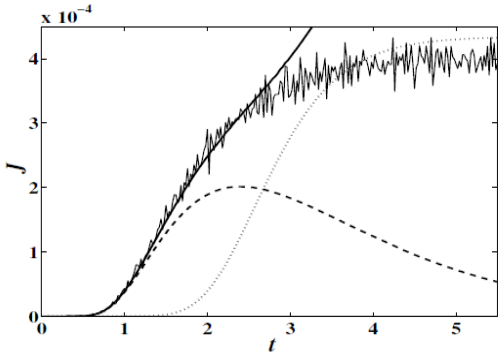

Fig. 2. Dynamics of the escape flux from the bottom of the Duffing potential (as in Fig. 1) to the top of the barrier corresponding to the Langevin equation (1) with D = 0.04. The flux was obtained from computer simulations (thin jagged line) and calculated: (i) by Eqs. (14) and (24) (thick solid line), (ii) by Eq. (14) (dashed line), and (iii) by the Shneidman theory, *i.e.* by Eq. (17) of [16] (dotted line).

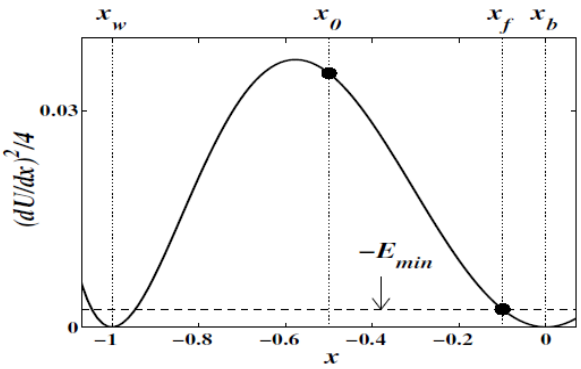

Fig. 3. The function $(dU(x)/dx)^2/4$ (thick solid line) for the Duffing potential (22) (see Fig. 1a). Dots indicate the points on the curve corresponding to x_0 = –0.5 and x_f = –0.1 (the corresponding values of x are indicated by the dotted lines and the labels x_0 and x_f; x_w and x_b are indicated analogously). The level $-E_{\min}$ (10) is indicated by the dashed line and the label.

A. The example of the Duffing potential

Consider first the Duffing potential (22) as a characteristic example. Let us choose the initial and final points of the transition to be the same to the case discussed in [22–24]:

$$x_0 = -0.5,\ \ x_f = -0.1. \tag{25}$$

Fig. 3 shows the function $(dU(x)/dx)^2/4$ for the Duffing potential (22). The points corresponding to x_0 and x_f (27) are indicated by dots. The most important feature of this example of $U(x)$ is the absence of the local minima of $(dU/dx)^2$ between x_w and x_b, apart from those at x_w and x_b themselves. This makes the minimum energy $E_{\min}$ (10) necessarily realized either at x_0 or at x_f. For the set (25), $E_{\min}$ is realized at x_f.

$$E_{\min} = -\frac{1}{4}\left(\frac{dU}{dx}\right)^2\Bigg|_{x_f} = -0.00245025\,. \tag{26}$$

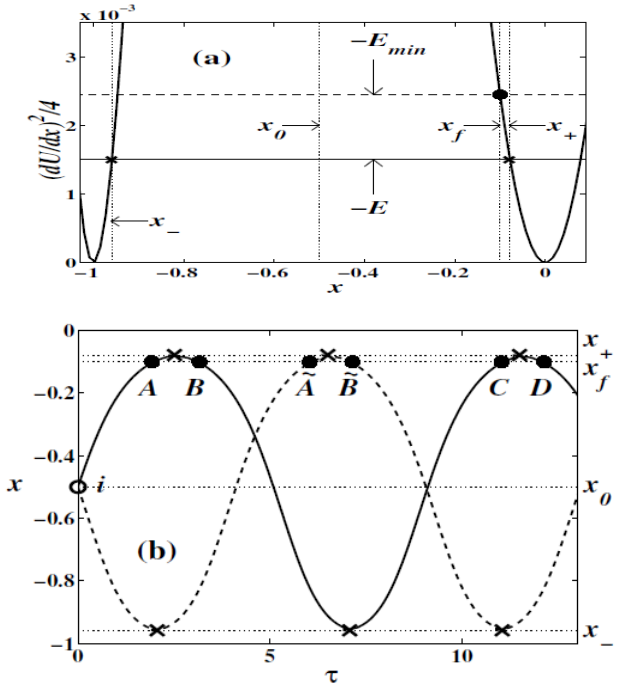

Fig. 4. (a) An example of the solution of Eq. (25) for $U(q)$ (22) at some arbitrarily chosen values $E < 0$. The function $(dU(x)/dx)^2/4$ in the relevant ranges is shown by the thick solid line. The level $-E$ is indicated by the thin solid line and corresponding label. The relevant graphic solutions are marked by crosses and their positions are indicated by the dotted lines and labels x_- and x_+ for the left and right solution, respectively. The positions x_0 and x_f of the initial and final points of the transition are also indicated by the dotted lines and corresponding labels. In addition, the point on the curve corresponding to x_f is marked by the dot. In our case, it determines $-E_{\min}$, which is shown by the dashed line and indicated by the corresponding label. (b) Extreme paths $[x(\tau)]$ corresponding to the given *energy* E as in (a) shown by the solid and dashed lines for the cases of the positive and negative initial velocity, respectively. The initial point is marked by the circle and additionally indicated by the label *i*. Possible final and turning points are marked by the dots and crosses, respectively. Different final points are additionally indicated by different labels: $A, \tilde{A}, B, \tilde{B}, \ldots$. The correspondence with the labels of different branches in Fig. 5 is given by Eq. (29).

Hence, the extreme paths corresponding to the range of energies $0 > E > E_{\min}$, possess one or more turning points. For a given energy, there are two different positions, which the turning points may have, x_+ and x_-. They are determined from the following equation:

$$E_{\min} = -\frac{1}{4}\left(\frac{dU}{dx}\right)^2, \tag{27}$$

so that $x_{+/-}$ is the closest root to $x_{f/0}$ among those situated on the same side from $x_{0/f}$ as $x_{f/0}$:

$$\left(x_{+/-} - x_{f/0}\right)\left(x_{f/0} - x_{0/f}\right) \geq 0 \tag{28}$$

(cf. Fig. 4a related to Eqs. (22) and (25)).

An extreme path with a given $E < 0$ may turn to x_- and x_+ any number of times. Let us resolve extreme paths by their topology, namely by overall number N of turns of $[x(\tau)]$ (*i.e.* the number of changes of the sign of velocity) and by the sign of the initial velocity multiplied by the sign of $x_f - x_0$. We shall use the labels like "N = 3, +". The sign of $[\dot{x}(x_f - x_0)]$ for $N = 0$ is necessarily "+" and will be omitted therefore. For the example shown in Fig. 4b, the labels should be put in correspondence with the extreme paths in the following way:

$$\begin{aligned}
&N = 0 \quad \leftrightarrow [i, A], \\
&N = 1,+ \leftrightarrow [i, B], \\
&N = 2,+ \leftrightarrow [i, C], \\
&N = 3,+ \leftrightarrow [i, D], \\
&N = 1,- \leftrightarrow [i, \tilde{A}], \\
&N = 2,- \leftrightarrow [i, \tilde{B}].
\end{aligned} \tag{29}$$

For each topology set above, the extreme path is uniquely defined. Moreover, it can be implicitly expressed *via* quadratures, analogously to the case with stationary points involved (cf. Eq. (17)). The *full time* along the extreme path with given topology and quasi-energy can be *explicitly* expressed via quadratures. To present respective expressions in a compact form, let us introduce three auxiliary times:

$$t_0 \equiv t_0(E) = t_{x_0 \leftrightarrow x_f},$$

$$t_+ \equiv t_+(E) = t_{x_f \leftrightarrow x_+},$$

$$t_- \equiv t_-(E) = t_{x_- \leftrightarrow x_0},$$

$$t_{a\leftrightarrow b} = \left|\int_a^b \frac{dq}{\dot{q}(E,q)}\right| = \operatorname{sign}\left[\frac{b-a}{x_f - x_0}\right]\int_a^b dq\, z(q,E), \tag{30}$$

where $z(q, E)$ is given by (17).

Then, for different topologies, the dependence of the full time along the extreme path on quasi-energy can be easily shown to be the following:

$$\begin{aligned}
&t_{N=0}(E) = t_0, \\
&t_{N=2n+1,+/-}(E) = t_0 + 2t_{+/-} + (N-1)(t_0 + t_+ + t_-), \\
&t_{N=2n+2,+/-}(E) = \pm t_0 + N(t_0 + t_+ + t_-), \\
&n = 0, 1, 2, \ldots
\end{aligned} \tag{31}$$

Fig. 5a shows all branches in the given ranges of t and E, calculated by Eq. (31) for the case corresponding to Fig. 3.

Let us turn now to one of the major purposes of the present section, namely to the calculation of action $S(t)$ for different branches of $t(E)$. Transforming from time to coordinate in the integral (6) using the relation $d\tau = dx/\dot{x}$ and the expression (9) for $\dot{x}$, one can explicitly express the action S corresponding to any branch of $t(E)$ *via* quadratures. In order to present the results in a compact form, we introduce the following auxiliary actions:

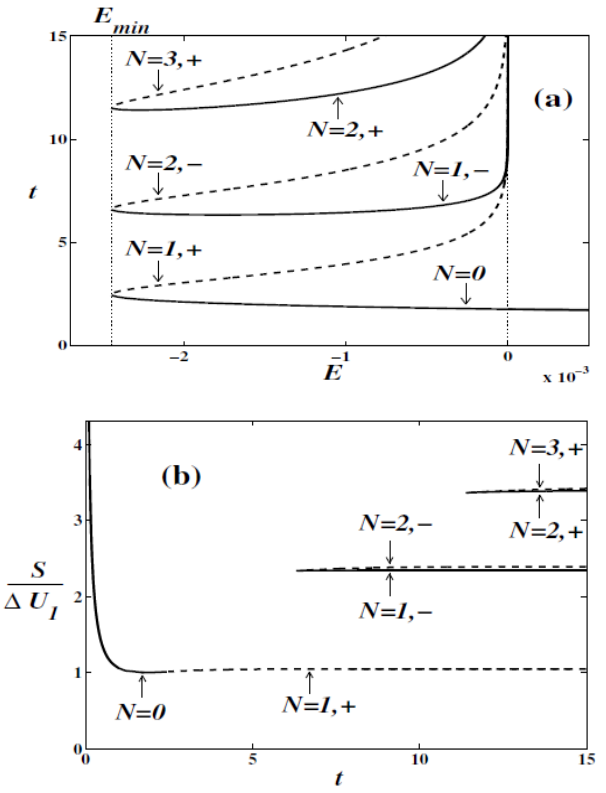

Fig. 5. (a) Calculated by Eq. (31) different branches of $t(E)$ for the case shown in Fig. 3. The branches corresponding to different topologies of the extreme path are shown by the thick solid/dashed lines. The labels indicate the numbers of turning points (in the form "$N = i$") and the sign of the initial velocity $\dot{x}(0)$ multiplied by the sign of $x_f - x_0$. (b) Calculated by Eq. (33) different branches of the action S (normalized by $\Delta U_1 \equiv U(x_f) - U(x_0) = 0.1044$) as functions of transition time are marked identically to the corresponding branches of $t(E)$ in (a).

$$S_0 \equiv S_0(E) = \int_{x_0}^{x_f} dq\, \eta(q,E),$$

$$S_1 \equiv S_1(E) = \int_{x_0}^{x_f} dq \left(\eta(q,E) - \frac{1}{2}\frac{dU}{dq} \right) = S_0 - \frac{1}{2}\Delta U_1,$$

$$\Delta U_1 \equiv U(x_f) - U(x_0),$$

$$S_+ \equiv S_+(E) = \int_{x_f}^{x_+} dq \left(\eta(q,E) - \frac{1}{2}\frac{dU}{dq} \right),$$

$$S_- \equiv S_-(E) = \int_{x_-}^{x_0} dq \left(\eta(q,E) - \frac{1}{2}\frac{dU}{dq} \right), \qquad (32)$$

where $\eta(q, E)$ is given by (20). Then $S(t)$ for different branches can be presented as follows:

$$S_{N=0}(t) = S_0,$$

$$S_{N=2n+1,+/-}(t) = S_0 + 2S_{+/-} + (N-1)(S_1 + S_+ + S_-),$$

$$S_{N=2n+2,+/-}(t) = S_0 + (\pm 1 - 1)S_1 + N(S_1 + S_+ + S_-),$$

$$n = 0, 1, 2, \ldots \qquad (33)$$

where the argument $E \equiv E(t)$ in S_0, S_1, S_+, S_- is to be taken for a given branch $S_{N,+/-}(t)$ as a solution of the equation

$$t = t_{N,+/-}(E), \qquad (34)$$

Here, the functions $t_{N,+/-}(E)$ are defined by (31). For the case of the Duffing potential (22) and the set of initial and final points (25), Eq. (34) has no more than one root, as can be shown using (31), (30) and (17). But generally speaking, Eq. (34) may have more than one root (cf. Figs. 6b, 8b and 9b), so that the function $S_{N,+/-}(t)$ is multi-valued then (cf. Figs. 8c, 9c and the inset in Fig. 6c).

Together with the auxiliary functions $z(q, E)$ and $\acute{\eta}(q, E)$ given by Eqs. (17) and (20), respectively, Eqs. (30)–(34) describe *via* quadratures all possible extreme paths and actions along them. We stress that this description is valid in a *general* case *i.e.* for arbitrary values of $U(x)$, t, x_0 and x_f.

Fig. 5b shows the results for different branches of $S(t)$ for the case corresponding to Fig. 3 (*i.e.* discussed in [22–24]). In particular, for $t = 8$ our results coincide with the numerical results for the branches "$N = 1$, –" and "$N = 1$, +" obtained in [22] and [23], respectively (the branch "$N = 2$, –" was omitted in [22–24]). At $t < t_0(E_{\min})$, the activation energy S_a coincides with the branch $S_{N=0}(t)$. It takes its lowest value, $\Delta U_1 \equiv U(x_f) - U(x_0)$, at $t = t_0(E = 0)$, which is the time of the noise-free relaxation from x_f into x_0. At $t = t_0(E_{\min})$, the branch "$N = 0$" passes continuously into the branch "$N = 1$, +", which constitutes S_a at all larger times. At $t \to \infty$, the corresponding asymptotic values of $S_{N,+/-}(t)$ reduce to

$$S_{N=2n+1,+}(t \to \infty) = U(x_b) - U(x_0) + \frac{N-1}{2}\Delta U,$$

$$S_{N=2n+1,-}(t \to \infty) = U(x_f) - U(x_w) + \frac{N-1}{2}\Delta U,$$

$$S_{N=2n+2,+/-}(t \to \infty) = \frac{1 \pm 1}{2}\Delta U_1 + \frac{N}{2}\Delta U,$$

$$n = 0, 1, 2, \ldots$$

$$\Delta U \equiv U(x_b) - U(x_w), \quad \Delta U_1 \equiv U(x_f) - U(x_0). \qquad (35)$$

It is obvious from (35) that $S(t \to \infty)$ may have a minimum only at the branches "$N = 1$, +" or "$N = 1$, – ". Therefore,

$$S_a(t \to \infty) = \min\left\{ U(x_b) - U(x_0), U(x_f) - U(x_w) \right\}. \qquad (36)$$

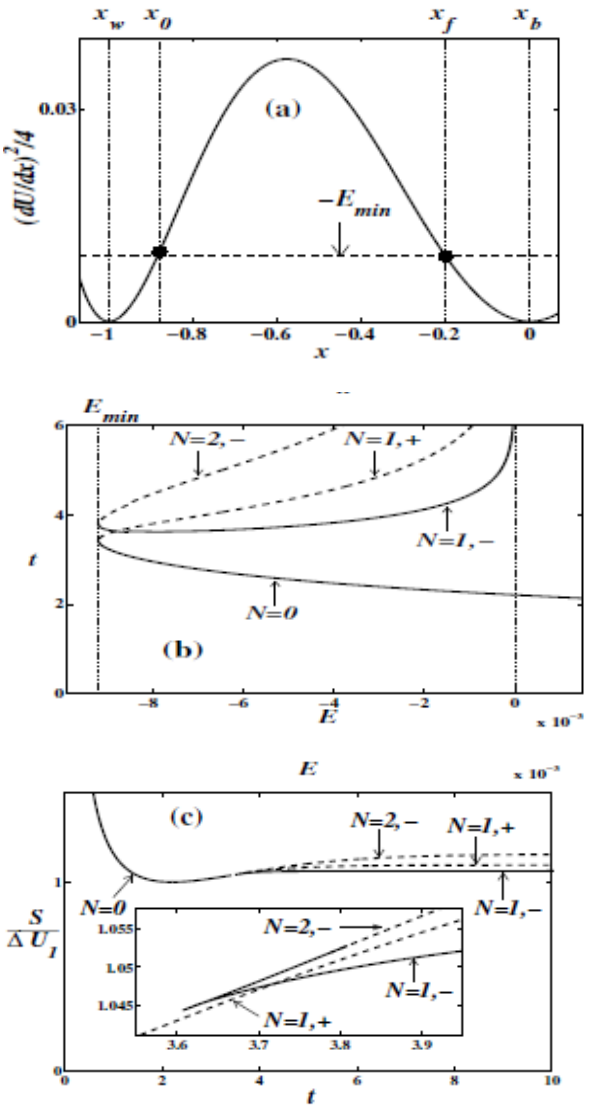

Fig. 6. Transition in the Duffing potential between the points with different positions from those corresponding to Figs. 3–5: $x_0 = -0.88$ and $x_f = -0.2$. (a), (b) and (c) are analogous to Figs. 3, 5a and 5b, respectively. The normalization in (c) is: $\Delta U_1 \equiv U(x_f) - U(x_{f0}) \approx 0.217676$. The inset in (c) shows the enlarged range of t and S where the jump-like switch between the branches $N = 1, +$ and $N = 1, -$ takes place. In its turn, it provides the switch of the topology of the MPTP.

In order for $S_a(t \to \infty)$ to be constituted by the branch "$N = 1, +$" rather than "$N = 1, -$", the following criterion is to be satisfied:

$$U(x_b) - U(x_0) < U(x_f) - U(x_w). \tag{37}$$

The criterion (37) was obtained in [23] on an intuitive ground and supported by numerical results. We note, however, that in a general case, domination of one of the branches at $t \to \infty$ may not necessarily guarantee the absence of a jump-like switch of the MPTP at some finite time. At some ranges of x_0 and x_f, the jump-like switch between the branches "$N = 1, +$" or "$N = 1, -$" may take place even for the Duffling potential considered here, as demonstrated by Fig. 6. In this case, the corresponding dependence $S_a(t)$ has a bend. Moreover, the flux changes its sign at the critical instant since the MPTPs corresponding to instants preceding and following the critical one approach x_f from different sides.

For other potentials, the switches may be much more pronounced and involve other branches, as shown in the next subsection.

B. Other characteristic cases

A picture of different branches of $t(E)$ and $S(t)$ may significantly differ from those described in the previous subsection if the function $(dU(x)/dx)^2$ has a local minimum in between its zeros. Consider as an example the following potential (Fig. 7):

$$U(x) = -x^5/5 + 0.8x^3/3 + 0.2x\,. \tag{38}$$

It is obvious from (9) that a path satisfying the equation of motion (11) slows down near the coordinate x_{lm} of the local minimum, similar to its slowing down near the bottom of the well x_w or the top of the barrier x_b.

Therefore, apart from the singularity corresponding to $E = 0$, one more singularity may appear in the dependence $t(E)$, which corresponds to $E = E_{lm}$.

Obviously, it forms only if either

$$E_{lm} = E_{\min}\,, \tag{39}$$

or

$$E_{lm} > E_{\min}\,. \tag{40}$$

is satisfied.

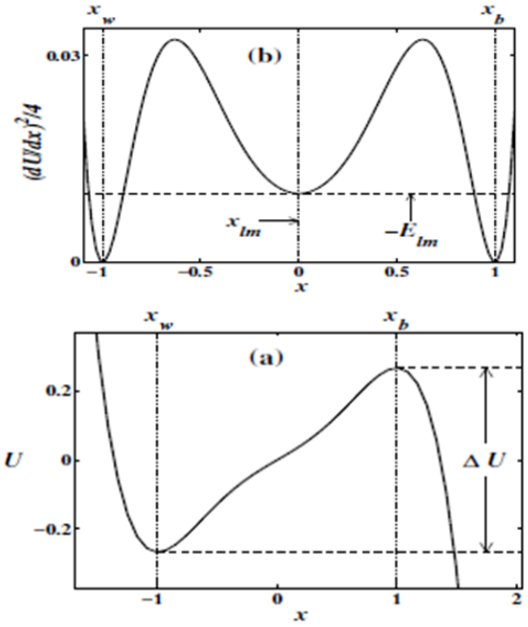

Fig. 7. (a) The potential $U(x) = -x^5/5+0.8x^3/3+0.2x$ and (b) the corresponding function $(dU(x)/dx)^2/4$. Positions of the bottom of the well and the top of the barrier are indicated by the dotted lines and labels x_w and x_b, respectively. The position and magnitude of the local minimum of $(dU(x)/dx)^2/4$ are indicated by the labels x_{lm} and $-E_{lm}$ and by the dotted and dashed lines, respectively.

Eq. (39) holds true if either the condition (41) (rather exceptionally) or, much more typically, the condition (42) is satisfied:

$$\left.\left(\frac{dU}{dx}\right)^2\right|_{x_{lm}} = \mu\,,$$

$$\mu \equiv \min\left(\left.\left(\frac{dU}{dx}\right)^2\right|_{x_0}, \left.\left(\frac{dU}{dx}\right)^2\right|_{x_f}, \left.\left(\frac{dU}{dx}\right)^2\right|_{x_{lm}^i}\right). \qquad (41)$$

Here, $x_{lm}^{(i)}$ are the coordinates of other possible local minima in the interval $]x_0,\ x_f[$, which may appear in a general case:

$$\left.\left(\frac{dU}{dx}\right)^2\right|_{x_{lm}} < \mu\,, \text{ while } x_{lm} \in]x_0, x_f[\qquad (42)$$

(see Fig. 8).

The case (40) is valid if (see Fig. 9)

$$\left.\left(\frac{dU}{dx}\right)^2\right|_{x_{lm}} < \mu\,, \text{ while } x_{lm} \notin [x_0, x_f] \qquad (43)$$

Let us first analyze the case (42) shown in Fig. 8 and corresponding to the validity of the expression (39), in more detail.

Any branch of $t(E)$ with $N \geq 1$ diverges at $E = 0$ and $E = E_{lm}$. Therefore, it necessarily has a minimum at some value $E_{N,+/-}^{(m)} < 0$ (cf. Fig. 8b):

$$\min_{E_{lm},0} t_{N\geq,+/-} \equiv t_{N,+/-}^{(m)} = t\left(E_{N,+/-}^{(m)}\right). \qquad (44)$$

On the other hand, any branch of $S(t)$ satisfies the following relation:

$$\frac{dS_{N,+/-}}{dt} = -E\,, \qquad (45)$$

where $E \equiv E(t)$ is the solution of Eq. (34). Eq. (45) is obtained similarly to Eq. (19) for the case when only one branch exists. Hence, any branch $S_{N\geq 1,+/-}(t)$ consists of two parts, both of which start in $S_{N,+/-}\left(t_{N,+/-}^{(m)}\right)$ (and monotonously increase as t increases (see Fig. 8c).

The lower part $S_{N,+/-}^{(low)}(t)$ corresponds to the energies in the range $[E_{N,+/-}^{(m)}, 0[$ and has the large-time asymptote (35). The upper part $S_{N,+/-}^{(up)}(t)$ corresponds to the energy range $]E_{\min}, E_{N,+/-}^{(m)}]$. As follows from (45), it has such large-time asymptote:

$$S_{N,+/-}^{(up)}(t \to \infty) = C_{N,+/-} - E_{lm}\, t\,, \qquad (46)$$

where $C_{N,+/-}$ is a constant having different values for different branches. A similar asymptote with the different constant corresponds to the branch $S_{N=0}(t)$.

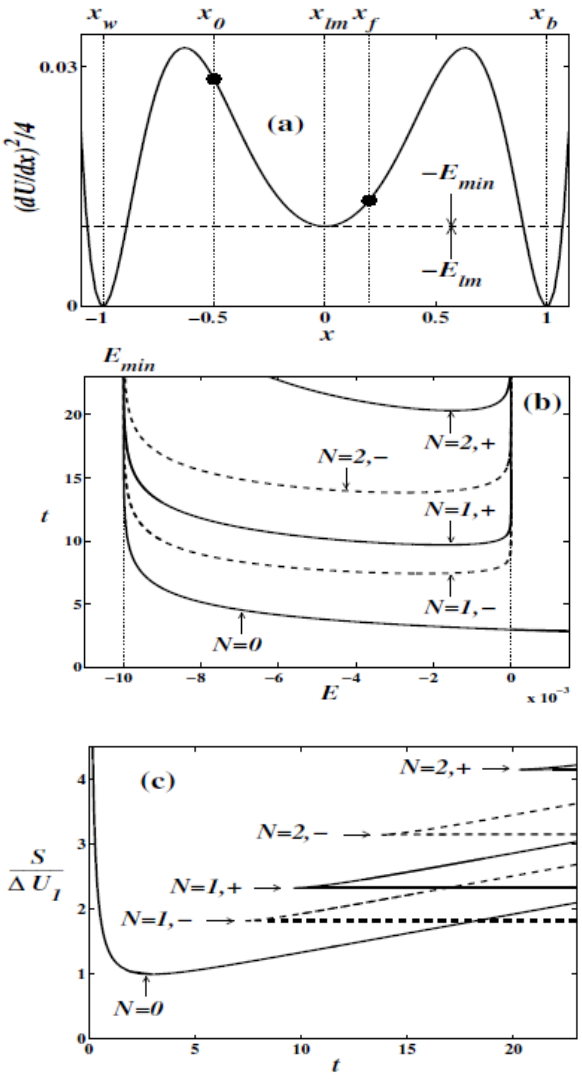

Fig. 8. Transition from $x_0 = -0.5$ *to* $x_f = 0.2$ in the potential (38) shown in Fig. 7a. As can be seen from (a), $E_{\min}$ coincides with the singularity energy E_{lm} corresponding to the local minimum of $(dU(x)/dx)^2/4$ shown by the dashed line and indicated by the label $-E_{lm}$. Other notations in (a) are analogous to those in Fig. 3. Panels (b) and (c) are analogous to Figs. 5a and 5b, respectively. The normalization in (c) is: $\Delta U_1 \equiv U(x_f) - U(x_0) \approx 0.16915$.

Therefore, the large-time asymptote of the activation energy S_a is described by the same expression (36) as for the case without the local minimum in $(dU(x)/dx)^2$, which corresponds to either "$N = 1, +$" or "$N = 1, -$" branch depending on whether the criterion (37) is satisfied.

At small times t, the activation energy S_a is constituted by the branch "$N = 0$". Unlike the case of a potential with $(dU/dx)^2$ having no relevant local minimum, the change of the topology of MPTP from "$N = 0$" to "$N = 1, +/-$" necessarily occurs jump-like since the branch $t_{N=0}(E)$ does not touch the branches $t_{N=0}(E)$ anywhere (Fig. 8b). As a result, the function $S_a(t) \equiv S_a = \min_{[N,+/-]}\{S_{N,+/-}\}(t)$ has a bend (cf. Fig. 8c).

The bend in $S_a(t)$ and the jump in the dependence of the MPTP on t are typically much more pronounced than in the case of a potential without the relevant local minimum of the $(dU(x)/dx)^2$ (cf. Figs. 8 and 6).

We have made computer simulations aiming to demonstrate: (i) a jump-like change of the MPTP topology with time and (ii) a reasonable agreement between the theoretically calculated MPTPs (and, more generally, extreme paths) and typical simulated trajectories. To this end, we have applied a very weak noise (with the intensity D = 0.01) to ensure narrow probability density distribution both in time and coordinate. If the initial and final points of the transition are taken as shown in Fig. 8, so that $U(x_f) > U(x_0)$, the statistics is so poor that hardly any transition path at such low value of D can be observed. To avoid this difficulty, we have simulated the reverse transition. We have shown that the extreme paths are just time-reversals of the paths for the direct transition. The dependence $S(t)/\Delta U_1$ is almost equivalent to that for the direct transition (see Fig. 8c) except for it is shifted down by 1:

$$\frac{S(t,\,0.2\to -0.5)}{\Delta U_1}=\frac{S(t,\,-0.5\to 0.2)}{\Delta U_1}-1\,. \qquad (47)$$

As a consequence, the probability density of the reverse transition exceeds that of the direct one by the huge factor $\exp(\Delta U_1/D) \approx \exp(16.9) \approx 2.22\times10^7$, so that the statistics is quite reasonable for the relevant range of time. Fig. 10 presents the results of simulations demonstrating the jump-like change of the MPTP topology as the transition time increases. Moreover, a reasonable agreement between our theory and simulations can be seen from Fig. 10. As follows from Fig. 8c, the actions for the branches "N = 0" and "N = 1, –" are equal each other at $t = t_e \approx 18.2$. This means that the MPTP topology at $t < t_e$ in the asymptotic limit $D \to 0$ is "N = 0" (no turning points), while it is "N = 1, –" (one turning point to the left from the initial point) at $t > t_e$. However, the value of the noise intensity D in real experiments necessarily differs considerably from zero. Generically, the values of the prefactor for different branches (topologies) differ from each other. This means in particular that the probability densities for intersecting branches (action *vs.* time) are equal at the time shifted from t_e by the value making the corresponding difference in the activation factors compensate the difference in the prefactors. This can be seen from comparison of Figs. 8c and 10. So, let us describe and analyze Fig. 10. For each of the two values of transition time t, 14.1 and 15.2, we have depicted six sequentially simulated transition paths. We have also drawn the respective theoretically calculated extreme paths corresponding to the branches "N = 0" and "N = 1, –". It can be seen from Fig. 10 that 5 of 6 simulated paths with t = 14.1 concentrate near the corresponding theoretical path without turning points, while 1 path concentrates near the theoretically calculated path with one turning point and negative initial velocity. In contrast, all 6 sequentially simulated paths for the case t = 15.2

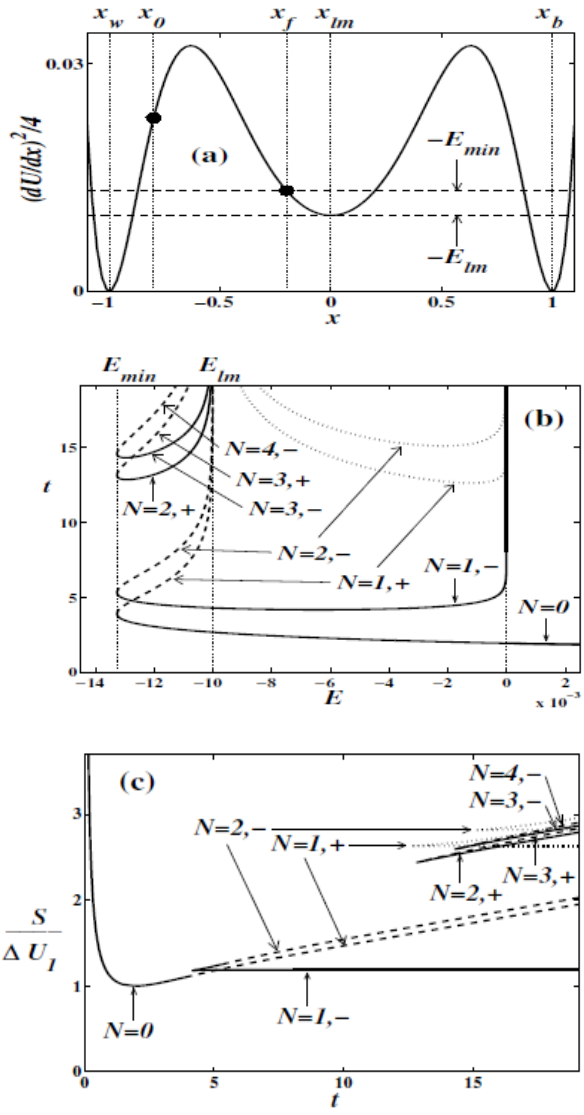

Fig. 9. This figure is analogous to Fig. 8 but the set of initial and final points of the transition differs: x_0 = –0.8, x_f = –0.2, so that $E_{\min} < E_{lm}$, as can be seen from (a) and (b). The normalization in (c) is: $\Delta U_1 \equiv U(x_f) - U(x_0) \approx 0.18893$. In (b) and (c), the branches relevant to MPTPs with right turning points situated to the right from the local minimum of $(dU/dx)^2$ (*i.e.* $x_+ > 0$) are shown by the thick dotted lines. Other branches are shown by the thick solid and dashed lines.

concentrate near the theoretical path with negative initial velocity and one turning point close to $x = x_w = -1$. One may conclude from these simulation results that the probability density for the noise intensity value D = 0.01 becomes equal for the two topologies of the path at $t = t_{e,ex}^{(D=0.01)}$ lying in between 14 and 15. Does the theory conform to this result? Calculation of the prefactor shows that the prefactor for the lower branch "N = 1, –" exceeds that for the branch "N = 0" by the factor of about 37 in the relevant time range (from 14 to 15). Therefore, the theoretical value of $t_{e,th}^{(D=0.01)}$ is shifted from $t_e \approx 18.2$ to the

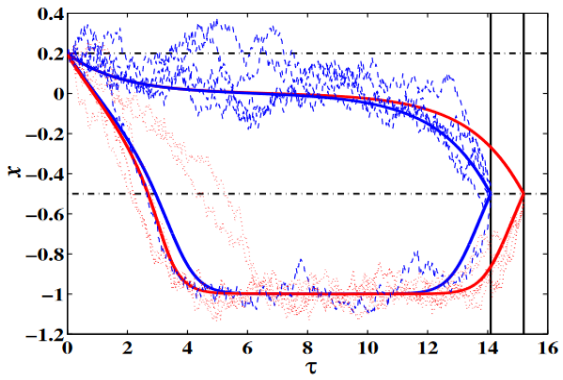

Fig. 10. Two series of sequentially measured transition paths [$x(\tau)$] of the stochastic system (1) with the potential $U(x)$ (38) (see Fig. 7a), the noise intensity $D = 0.01$, the initial point $x(0) \equiv x_0 = 0.2$ and the final point $x(t) \equiv x_f = -0.5$ for two values of transition time: $t = 14.1$ (blue dashed lines) and $t = 15.2$ (red dotted lines). x = 0.2 and x = –0.5 are shown by the black dash-dotted lines. $\tau = 14.1$ and $\tau = 15.2$ are marked by the black solid lines. The theoretical extreme paths corresponding to the branch "$N = 0$" and the lower part of the branch "$N = 1, -$" (cf. Fig. 8c) are shown by the thick solid blue and red lines for $t = 14.1$ and $t = 15.2$, respectively. (Color online)

value providing approximately the excess of the activation factor for the branch "$N = 0$" over that for the branch "$N = 1, -$" by the factor of 37. Looking at Fig. 8c, we conclude that this value is $t_{e,th}^{(D=0.01)} \approx 14.6$, that nicely conforms to the simulation results. Fig. 10 also demonstrates that the simulation paths concentrate near the theoretically calculated extreme paths, first of all near the MPTP.

Finally, we characterize the case (40) (which requires (43) to hold true) shown in Fig. 9. It provides a richer variety of branches than the case (38) since Eq. (34) may have more solutions in this case due to the range of energies [$E_{\min}$, E_{lm}[coming into play. On the other hand, the new types of solutions may constitute S_a only in a narrow range of t close to $t_{N=0}(E_{\min})$ (cf. Fig. 9c). Therefore, the branch "$N = 0$" in the case shown in Fig. 9 constitutes S_a at $t < \tau_1 \approx 4$. Then it passes continuously into the branch "$N = 1, +$" with the turning point x_+ situated on the same side from x_{lm} as x_f. At $t = \tau_2 \approx 5$, the latter branch switches jump-like to the branch "$N = 1, -$" with the turning point x_+ situated far on the other side from x_{lm}. Hence, both the bend in $S_a(t)$ and the jump in MPTP are as pronounced as in the case (42).

4. Conclusions

Using the path-integral approach, we have derived a complete solution of the problem of noise-induced escape of a 1D overdamped potential system from a potential well at short time scales for arbitrary potentials. The results obtained here differ from the former predictions by Shneidman. The simulation results have good agreement with our theory for the time range preceding the onset of the quasi-stationary stage. We have also developed a detailed theory of the transition between the points, neither of which is the bottom of the well. We have classified possible cases. In particular, if the potential in between the initial and final points of the transition does not possess extrema, the activation energy vs. time necessarily has a minimum at the time equal to the time of the purely dynamic transition from the point with a higher value of the potential to the another one. Besides, as time increases, the MPTP with no turning point may change jump-like at certain time t_e to the MPTP with one turning point. At this, the activation energy S *vs*. time t has a distinct bend at $t = t_e$.: a rather sharp growth of S with t changes jump-like at $t = t_e$ to almost a plateau. The theory conforms well to our computer simulations. Our results may be relevant to Josephson junctions, levitating nanoparticles in optical traps, ionic channels, chemical reactions of a single molecule and chemical-physical systems.

Acknowledgements

We dedicate this work to Prof. Emmanuil Iosifovich Rashba.

References

1. Risken H. The *Fokker-Planck Equation. Methods of Solutions and Applications*. 2nd ed. Springer-Verlag, Berlin, 1992.
2. Likharev K.K. *Dynamics of Josephson Junctions and Circuits*. Taylor & Francis Group, LLC, Boca Raton, London, New York, 1986.
3. Van Exter M.P., Willemsen M.B., Woerdman J.P. Polarization fluctuations in vertical-cavity semi-conductor lasers. *Phys. Rev. A.* 1998. **58**. P. 4191. https://doi.org/10.1103/PhysRevA.58.4191.
4. Ornigotti L., Filip R. Uncertainty-induced instantaneous speed and acceleration of a levitated particle. *Sci. Rept.* 2021. **11**. P. 18185. https://doi.org/10.1038/s41598-021-97663-z.
5. Gonzalez-Ballestero C., Aspelmeyer M., Novotny L., Quidant R., Romero-Isart O. Levitodynamics: Levitation and control of microscopic objects in vacuum. *Science*. 2021. **372**. P. 6564. https://doi.org/10.1126/science.abg3027.
6. Berezhkovskii A.M., Pustovoit M.A and Bezrukov S.M. Channel-facilitated membrane transport: Transit probability and interaction with the channel. *J. Chem. Phys*. 2002. **116**. P. 9952. https://doi.org/10.1063/1.1475758; Average lifetimes in the channel: Channel-facilitated membrane transport. 2003. **119**. P. 3943. https://doi.org/10.1063/1.1590957.
7. Zheng J., Trudeau M.C. *Handbook of Ion Channels*. CRS Press, 2015.
8. Kaufman I.K., McClintock P.V.E., Eisenberg R.S. Coulomb blockade model of permeation and selectivity in biological ion channels. *New J. Phys*. 2015. **17**. 083021. https://iopscience.iop.org/article/10.1088/1367-2630/17/8/083021.
9. Kramers H.A. Brownian motion in a field of force and the diffusion model of chemical reactions. *Physics*.

1940. **7**, No 4. P. 284–304. https://doi.org/101016/S00312-8914(40)90098-2.
10. Lu H.P., Xun L., Xie X.S. Single-molecule enzyme-tic dynamics. *Science*. 1998. **282(5395)**. P. 1877–1882. https://doi.org/10.1126/science.282.5395.1877.
11. Barkai E., Jung Y., and Silbey R. Theory of single-molecule spectroscopy: Beyond the ensemble average. *Ann. Rev. Phys. Chem*. 2004. **55**. P. 457–507. https://doi.org/10.1146/ annurev.physchem.55.111803.143246.
12. Li Y., Debnath D., Ghosh P.K., and Marchesoni F. Nonlocality of relaxation rates in disordered landscapes. *J. Chem. Phys*. 2017. **146**. 084104. https://doi.org/10.1063/1.4976844.
13. Einstein A. Über die von der molekularkinetischen Theorie der Wärme geforderte Bewegung von in ruhenden Flüssigkeiten suspendierten Teilchen. *Annalen der Physik*. 1905. **17**. P. 549–560. https://doi.org/10.1002/andp.19053220806.
14. Einstein A. Zur Theorie der Brownschen Bewegung. *Annalen der Physik*. 1906. **19**. P. 371–381. https://doi.org/10.1002/andp.19063240208.
15. Smoluchowski M. Über Brownsche Molekularbewegung unter Einwirkung äußerer Kräfte und deren Zusammenhang mit der verallgemeinerten Diffusionsgleichung. *Annalen der Physik*. 1916. **353**, No 24. P. 1103–1112. https://doi.org/10.1002/andp.19163532408.
16. Shneidman V.A. Transient solution of the Kramers problem in the weak noise limit. *Phys. Rev. E*. 1997. **56**. P. 5257. https://doi.org/10.1103/PhysRevE.56.5257.
17. Feynman R.P. and Hibbs A.R. *Quantum Mechanics and Path Integrals*. McGraw-Hill, New York, 1965.
18. Gelfand I.M. and Yaglom A.M. Integration in functional spaces and its applications in quantum physics. *J. Math. Phys*. 1960. **1**, No. 1. P. 48–69. https://doi.org/10.1063/1.1703636.
19. Rattray K.M. and McKane A.J. Stationary proba-bility distribution for a particle subject to coloured noise. *J. Phys. A: Math. Gen*. 1991. **24**, No 18. P. 4375. https://iopscience.iop.org/article/ 10.1088/0305-4470/24/18/023/pdf.
20. Lehmann J., Reimann P., Hanggi P. Surmounting oscillating barriers: Path-integral approach for weak noise. *Phys. Rev. E*. 2000. **62**. P. 6282. https://doi.org/10.1103/PhysRevE.62.6282.
21. Luchinsky D.G., McClintock P.V.E., Dykman M.I. Analogue studies of nonlinear systems. *Rept. Prog. Phys*. 1998. **61**, No 8. P. 889. https://iopscience.iop.org/article/10.1088/0034-4885/61/8/001.
22. Vugmeister B.E., Botina J., and Rabitz H. Nonstationary optimal paths and tails of prehistory probability density in multistable stochastic systems. *Phys. Rev. E*. 1997. **55**. P. 5338. https://doi.org/10.1103/PhysRevE.55.5338.
23. Mannella R. Comment on "Nonstationary optimal paths and tails of prehistory probability density in multistable stochastic systems". *Phys. Rev. E*. 1999. **59**. P. 2479. https://doi.org/10.1103/PhysRevE.59.2479.
24. Vugmeister B.E., Botina J., and Rabitz H. Reply to "Comment on 'Nonstationary optimal paths and tails of prehistory probability density in multistable stochastic systems'". *Phys. Rev. E*. 1999. **59**. P. 2481. https://doi.org/10.1103/PhysRevE.59.2481.
25. Dykman M.I., McClintock P.V.E., Smelyanskiy V.N., Stein N.D., and Stocks N.G. Optimal paths and the prehistory problem for large fluctuations in noise-driven systems. *Phys. Rev. Lett.* 1992. **68**. P. 2718. https://doi.org/10.1103/PhysRevLett.68.2718.
26. Soskin S.M., Sheka V.I., Linnik T.L., Mannella R. Escapes and transitions in overdamped systems on short times: General solution. In *Unsolved Problems of Noise*. Ed. L. Reggiani, C. Penneta, V. Akimov, E. Alfinito, M. Rosini. American Institute of Physics, Melville, NY, USA. 2005. *AIP Conf. Proc*. 2005. **800**, No 1. P. 262–269.
27. Stocks N.G. private communication.
28. Smelyanskiy V.N. and Dykman M.I. Optimal control of large fluctuations. *Phys. Rev. E*. 1997. **55**. P. 2516. https://doi.org/10.1103/PhysRevE.55.2516.
29. Vugmeister B. E. and Rabitz H. Cooperating with nonequilibrium fluctuations through their optimal control. *Phys. Rev. E*. 1997. **55**. P. 2522. https://doi.org/10.1103/PhysRevE.55.2522.
30. Soskin S.M., Sheka V.I., Linnik T.L., Mannella R. Noise-induced transitions in overdamped systems: short times. *Noise in Complex Systems and Stochastic Dynamics*, Eds. L. Schimansky-Geier, D. Abbott, A. Neiman and C. Van den Broeck, *Proc. Series. SPIE*, Washington. 2003. **5114**. P. 289–300.
31. Elsgolc L.E. *Calculus of Variations*. Pergamon Press, London. 1961.
32. Soskin S.M. Most probable transition path in an overdamped system for a finite transition time. *Phys. Lett. A*. 2006. **353**. P. 281–290. https://doi.org/10.1016/j.physleta.2005.12.110.
33. Landau L.D., Lifshitz E.M. *Mechanics*. Pergamon Press, London, 1976.

Authors and CV

Stanislav Soskin, Doctor of sciences, Leading scientific researcher at the Theoretical Physics Department, V. Lashkaryov Institute of Semiconductor Physics, NAS of Ukraine, was born in 1960. He defended his Ph.D. thesis in Physics and Mathematics (Semiconductor Physics) in 1988 at Institute of Semiconductors, Kyiv, Ukraine. He defended his D.Sci. thesis in Physics and Mathematics (Theoretical Physics) in 2011 at Bogolyubov Institute of Theoretical Physics (Kyiv, Ukraine). S. Soskin authored 90 publications, with an H index of 20. The area of his scientific interests includes stochastic and nonlinear dynamics and their manifestation in physics, nano/micro-electromechanical resonators, semiconductor superlattices. ORCID: https://0000-0003-1089-5867.
E-mail: stanislav.soskin@gmail.com

There are many links binding S. Soskin with Prof. E.I. Rashba: apart from being born in the same city (Kyiv) and living in the childhood in the same house, S.M. Soskin was closely related to Rashba's disciples: V.I. Sheka, V.O. Kochelap, and V.I. Melnikov, while since 2001 Soskin often communicated with Rashba on various scientific issues. On the top of that, Soskin's father (Prof. Marat S. Soskin) was in close friendly relations with Rashba for more than 60 years and often discussed with the son wise statements by Rashba.

Valentin Sheka (1934-2021), Prof., was Senior scientific researcher in Theoretical Physics Department of V. Lashkaryov Institute of Semiconductor Physics, NAS of Ukraine. He defended his Ph.D. thesis in Physics and Mathematics (Solid State Physics) in 1961 at Institute of Semiconductors, Kyiv, Ukraine. He is a well-known expert in solid state theory, especially in application of symmetry methods and of the variational method to the solid-state physics, in particular he derived fundamental results jn photo-transitions with a participation of spin. V. Sheka was one of the favorite disciples of E.I. Rashba and their collaboration continued until he passed away in 2021. In the end of the 50^{th} and in the 60^{th}, he participated together with his mentor in laying foundations of the methodology of using symmetry approaches in solid state physics, especially in problems related to the spin-orbit coupling. For these works, Rashba and Sheka became laureates of the S.I. Pekar Prize of the National Academy of Science of Ukraine in 2005. In 2017, the book "Method of Invariants in Semiconductor Physics" by V.I. Sheka and T.L. Linnik was published. He also authors about 100 other publications.

Tetyana Linnik, Senior scientific researcher at the Theoretical Physics Department of V. Lashkaryov Institute of Semiconductor Physics, NAS of Ukraine, was born in 1971. She defended her Ph.D. thesis in Physics and Mathematics (Solid State Physics) in 2002 at V. Lashkaryov Institute of Semiconductors, Kyiv, Ukraine. She is an author of more than 30 publications. T. Linnik specializes in the theory of semiconductor nanostructures, including effects related to the presence of deformation. Besides, she is an expert in theoretical studies of noise-induced transitions by means of path-integral methods.
https://orcid.org/0000-0002-5498-9702.
E-mail: tetiana.linnik@tu-dortmund.de

Riccardo Mannella, Author 4, Professor, Physics Department, Pisa University, was born in 1960. He defended his Ph.D. thesis in Physics in 1990 at Pisa University. Riccardo Mannella authored over 190 publications. R. Mannella authored over 190 publications, with an H-index (Scopus) of 36. The area of his scientific interests includes nonlinear stochastic physics, complex and chaotic systems. E-mail: riccardo.mannella@unipi.it;
https://orcid.org/0000-0002-0049-2506.

Author' contribution

Soskin S.M.: formal analysis, investigation, writing original draft, writing – review & editing, project administration.

Sheka V.I.: conceptualization, methodology, validation, investigation – numerical calculations, writing – original draft.

Linnik T.L.: investigation – numerical calculations, visualization, writing – original draft, writing – review & editing.

Mannella R.: investigation – computer simulations, resources, writing – review & editing.

Короткочасна динаміка виходів і переходів, стимульованих шумом у наддемпфованих системах
С.М. Соскін, В.І. Шека, Т.Л. Лінник, R. Mannella

Анотація. Використовуючи метод інтегралів по траєкторіях, ми розробили загальний алгоритм розв'язку задачі про динаміку ймовірності викликаного шумом виходу або переходу наддемпфованої одновимірної потенціальної системи на часових масштабах порядку часу динамічної релаксації. Результати сильно відрізняються від отриманих раніше іншими методами. Комп'ютерне моделювання підтверджує справедливість нашої теорії у відповідному часовому діапазоні. Отримані результати можуть становити інтерес для досліджень джозефсонівських контактів, левітуючих наночастинок в оптичних пастках, іонних каналів, хімічних реакцій та хіміко-фізичних систем.

Ключові слова: одновимірна потенціальна система; короткочасна динаміка; вихід, викликаний шумом; наддемпфована система; метод інтегралів по траєкторіях.